

# Time-varying three-dimensional vector field visualisation for the analysis of retrobulbar fat mobility during eye motion

Charl P. Botha<sup>1</sup>, Thijs de Graaf<sup>2</sup>, Ronald Root<sup>2</sup>, Piotr Wielopolski<sup>3</sup>  
Sander Schutte<sup>2</sup>, Frits H. Post<sup>1</sup>, Frans C.T. van der Helm<sup>2</sup>, Huib Simonsz<sup>4</sup>

Data Visualisation<sup>1</sup> and Man-Machine Systems<sup>2</sup>, TU Delft  
Radiology<sup>3</sup> and Ophthalmology<sup>4</sup>, Erasmus Medical Centre Rotterdam  
Corresponding author: cpbotha@ieee.org

## Abstract

Retrobulbar fat, or the fat behind the eyeball, plays an important role in eye motion. In order to gain a better understanding of retrobulbar fat mobility during eye motion, MRI datasets of the eyes of a healthy subject were acquired during seven different gaze directions. The Demons deformable registration algorithm was used to derive time-dependent three-dimensional deformation vector fields from these datasets. Visualisation techniques were applied to these datasets in order to investigate fat mobility in specific regions of interest. In two of the three regions of interest, fat moved half as fast as the embedded structures. In other words, when the muscles and the optic nerve that are embedded in the fat move, the fat partly moves along with these structures and partly flows around them. This raises compelling research questions.

## 1 Introduction

The human eye is able to rotate at up to 1000 per second and has an angular range of 100° horizontally and 90° vertically. It is able to do all of this with almost no translation of the centre of the eyeball. Eye movement is driven by six eye muscles. The upper image in figure 1 shows the medial and lateral rectus muscles that are responsible for horizontal motion. The lower image shows the superior and inferior rectus muscles that are responsible for vertical motion. The oblique eye muscles are able to perform torsionary eye motion.

The exact nature and parameters of the mechanics supporting eye movement is still not entirely clear. For example, as part of the “Active Pulley

Hypothesis”, it was proposed that the connective tissue bands connecting the horizontal rectus muscles to the inside wall of the orbit, first described by Tenon in 1816 and later called “pulleys” by Miller in 1989 [1], are responsible for the fact that these muscles show a specific inflection or bending point during vertical eye motion [2].

However, in recent work it was demonstrated with a finite element analysis model of the eye as well as clinical observation that these muscles show this inflection point without any connective tissue structures [3, 4]. It has also become clear that the retrobulbar fat, i.e. the fat behind the eyeball, plays an important role in the mechanics of eye movement. Currently, relatively little is known about the mobility of this fat during eye movement.

This paper documents our initial efforts on studying the mobility of the retrobulbar fat during eye motion. Inspired by previous work in this regard [5], we applied a deformable registration technique to multiple time-dependent MRI datasets of a healthy subject. The resultant time-varying three-dimensional deformation vector fields were used to measure and visualise the motion of retrobulbar eye-fat during eye movement.

Our contribution lies in the fact that this study, a collaboration between computer scientists, biomechanical engineers and clinicians, applies advanced visualisation techniques to a real biomedical problem and comes to relevant conclusions about three-dimensional retrobulbar fat mobility during eye motion. These conclusions confirm previous work performed on two-dimensional data and lead to interesting new questions. In addition, we demonstrate that using interactive advection volumes is an effective way of investigating three-dimensional time-varying deformation vector fields.

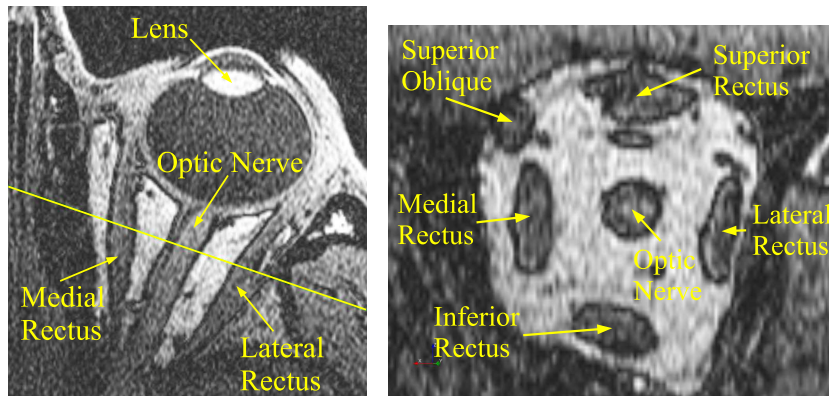


**Figure 1:** The left image is of an axial slice of an MRI dataset of an eye showing the medial and lateral rectus muscles and the optic nerve. The white material surrounding the eye-muscles is retrobulbar fat. On the left of the image, part of the nose is visible. The right image shows a slice orthogonal to that, intersecting at the diagonal line shown on the axial slice. This orthogonal slice shows the superior and inferior rectus muscles as well as the superior oblique muscle. The inferior oblique muscle is not visible in this image, but is diagonally opposite to the superior oblique.

The rest of this paper is structured as follows: section 2 contains a brief summary of work related to this study. Section 3 explains the methods and tools we used for our study. In section 4 we show the results of our analysis and in section 5 we summarise our findings and indicate avenues for future work.

## 2 Related Work

In [5], the 2-D Lucas and Kanade optical flow algorithm is extended to three dimensions and applied to various test datasets as well as an MRI dataset of an eye during different directions of gaze. Our study makes use of the Demons deformable registration algorithm [6], as this is a popular choice for the non-rigid registration of MRI datasets. In addition, we make use of advection to quantify the fat motion. Another important difference is that [5] focuses more on the validation of the actual technique rather than an investigation of actual fat mobility. It does come to the conclusion that the retrobulbar fat “deforms like a liquid and less like a solid”. It also describes how the fat fills the area behind the moving optic nerve from above and below during horizontal motion. This is described as “this tissue [the fat], thus, fills the vacuum left by the nerve, as behind a spoon moving through syrup”.

In a previous two-dimensional study based on MRI data, it was determined that the retrobulbar fat surrounding the optic nerve moves horizontally only 54% as fast as the optic nerve itself during horizontal eye motion [7].

## 3 Methods

### 3.1 Acquisition

MRI volume datasets were acquired of the eyes of a healthy subject in seven different directions of gaze. The T1-weighted scans were acquired on a 1.5 Tesla General Electric MRI scanner. We made use of a mobile transceiver surface coil for higher resolution. This resulted in seven  $512 \times 512 \times 84$  MRI datasets with resolution  $0.273 \times 0.273 \times 0.5\text{mm}$ . For the deformation analysis, four of the datasets were used: the central direction of gaze, and three directions of gaze to the left at respectively  $14^\circ$ ,  $24^\circ$  and  $33^\circ$ .

### 3.2 Software tools

The Delft Visualisation and Image processing Development Environment, or DeVIDE, is a software environment for the rapid prototyping and application of visualisation and image processing techniques [8]. It makes use of the VTK [9] and ITK [10] software toolkits. Its primary user interface is a graphical canvas where boxes, representing functional modules or algorithms, can be placed. These boxes can be connected together to form functional networks. This is similar to other packages such as OpenDX [11] and AVS [12]. All processing and visualisation described in this paper was performed using the DeVIDE software.

### 3.3 Pre-processing

During image acquisition, the subject’s head was fastened to the MRI patient table with surgical tape in order to minimise head motion during the relatively long total scan duration. Acquisition takes approximately one minute per direction of gaze, but significant time is spent on setup actions between directions of gaze. In spite of the head fixation, slight subject head motion did occur. In order to eliminate this rigid head motion in the acquired data, corresponding sets of six bony landmarks each were defined in all datasets. The datasets representing the central direction of gaze was chosen as the reference. Rigid transformations, optimal in a least squares sense, were derived to map the three other landmark sets onto the reference set [13]. These transformations were used to resample the data volumes with cubic interpolation, thus eliminating most of the rigid motion.

A number of points defining the extrema of the left eye were selected in all datasets. The datasets were cropped to the axis-aligned bounding box surrounding these points in order to save on computation time.

### 3.4 Deformable registration

The Demons deformable registration algorithm [6] was used to determine the three three-dimensional vector datasets describing the deformation from the central direction of gaze through the three directions of gaze to its left, i.e. from 0 to 14°, from 14 to 24° and from 24 to 33°. Because the Demons algorithm is based on the assumption that corresponding points in the source and target datasets have the same intensity, the intensity values of each pair of datasets were normalised by using a histogram matching implementation from ITK [10].

### 3.5 Visualisation and measurement

The resulting vector fields can be visualised with traditional flow visualisation techniques such as glyphs or streamlines, but these techniques all suffer from the problems plaguing most three-dimensional flow visualisation techniques: occlusion, lack of directional cues, lack of depth cues and visual complexity. To compound matters, we are dealing with time-varying data. In spite of all this, existing techniques are a great help in localising regions of interest that can be examined in more depth with other techniques.

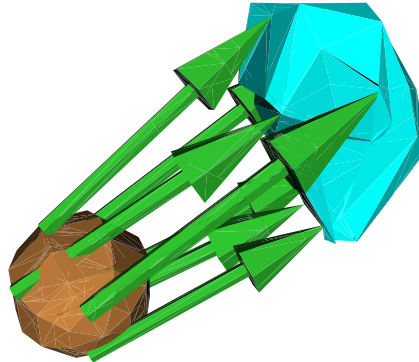


**Figure 2:** The sub-volume advection, shown for a single spherical region of interest and for a single time-step. The sphere on the left is the original as selected by the user. The object on the right has been deformed by the current vector field. The vector field associated with the next time step will subsequently be applied to the vertices of the deformed region of interest.

In our case, we were interested in the fat deformation in three specific areas. We chose to apply user-guided advection volumes. Small sub-volumes are placed in regions of interest. Each sub-volume is defined by a containing polygonal surface. Points are placed within the interior of this sub-volume at a user-definable density. Each of these points, as well as the vertices defining the containing surface, can then be displaced by the interpolated deformation vectors at their various positions, for that time-step. Figure 2 shows this process for a single time-step and a single spherical volume. The deformed volume, shown on the top right, is used as the initial volume for the next vector field. In this way we can keep on deforming the volume as many times as we have vector datasets.

DeVIDE allows one to place any number of these volumes in an MRI dataset. As soon as a volume is placed, it is advected through all loaded vector fields and the initial volume as well as all deformed volumes for that point are visualised. An already placed volume can also be moved. This allows for the interactive exploration of a time-varying deformation vector field. Figure 3 shows an example of such an interactive visualisation with three initial volumes advected over four vector datasets.

## 4 Results

Three regions were selected for closer inspection:

1. The region between the medial rectus and the eyeball. As the eye turns anti-clockwise, this

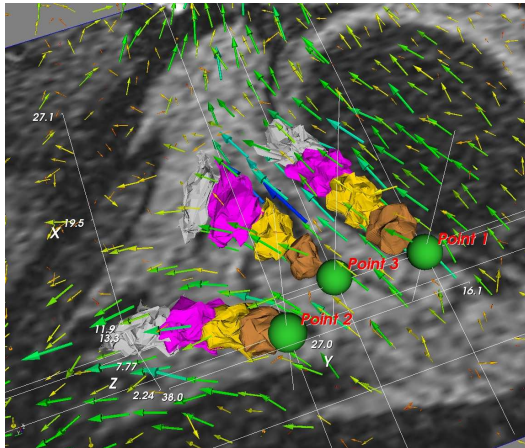


**Figure 3:** A visualisation with three advection volumes over four time-varying vector fields. An axial MRI slice can be seen in the background.

muscle “rolls up” onto the eyeball.

2. Around the optic nerve right behind the eye.
3. The region at the apex where the eye-muscles and optic nerve meet, about 25mm behind the eyeball.

In all of these regions a number of spherical volumes were placed and advected with the three deformation vector fields. In the first case, i.e. between the medial rectus and the eyeball, the resolution of the datasets and of the resultant vector fields was too low to make any kind of judgement.

In the second case, seven small spherical volumes were placed directly behind the eyeball: six surrounding the optic nerve at regular angles and one in the optic nerve itself. As the left eye turns anti-clockwise, the optic nerve moves medially, i.e. in the direction of the nose. The fat surrounding the optic nerve moved in the same direction and primarily transversally. What was significant, is that the fat moved only half as fast as the optic nerve.

In the third case, advected volumes indicated that the fat moved primarily in the same direction as the muscles. Once again, the fat moved half as fast as the muscles.

## 5 Conclusions and future work

In this paper we have documented a study of retrobulbar fat dynamics based on multiple MRI datasets acquired of a healthy subject’s eyes during different directions of gaze. Time-varying three-dimensional vector fields were generated by making use of the

Demons deformable registration technique. These vector fields were visualised with the DeVIDE software system and analysed by making use of advection volumes.

With these methods, it was determined that directly behind the eye and at the apex where the muscles and the optic nerve meet, fat moves 50% slower than respectively the optic nerve and the muscles embedded in it. In other words, retrobulbar fat moves partly along with these moving structures, but it partly flows around them as well. This confirms, in three dimensions, the results of a previous two-dimensional study [7] and raises an interesting new question: does this 50% principle apply to all structures in the retrobulbar fat, and if so, why?

In future work, we plan to continue this research on higher resolution data acquired with a 3 Tesla MRI scanner. Very importantly, the fixation of the subject’s head during scanning has to be improved. The rigid motion can be eliminated as explained in this paper, but it is desirable to minimise head motion during the acquisition phase. In the words of Dr Michael Vannier during his SPIE Medical Imaging 2004 keynote: *Good imaging beats good image processing*. For the residual motion that still might occur, it is important to localise easily identifiable rigid landmarks during acquisition.

The interactive advection volumes constitute an effective method to visualise and quantify local fat deformation. However, a more global visualisation technique would be useful to help understand the complex retrobulbar fat deformation fields. One interesting idea is the development of a realistic fluid flow simulation and visualisation that uses the derived vector fields as basis, so that the fat deformation can be studied in pseudo real-time. We will also continue our investigation of alternative techniques for the visualisation of local deformation.

## References

- [1] J. Miller, “Functional anatomy of normal human rectus muscles,” *Visual Research*, vol. 29, pp. 223–240, 1989.
- [2] J. L. Demer, “The orbital pulley system: a revolution in concepts of orbital anatomy,” *Annals of the New York Academy of Sciences*, vol. 956, pp. 17–33, 2002.
- [3] S. Schutte, S. van den Bedem, F. Keulen, F. T. van der Helm, and H. Simonsz, “First application of finite-element (fe) modeling to investigate orbital mechanics,” in *Proceedings of the*

*Association for Research in Vision and Ophthalmology (ARVO) Annual Meeting*, 2003.

- [4] S. Schutte, “Orbital mechanics and improvement of strabismus surgery,” Master’s thesis, Delft University of Technology, 2005.
- [5] M. D. Abramoff and M. A. Viergever, “Computation and visualization of three-dimensional soft tissue motion in the orbit,” *IEEE Transactions on Medical Imaging*, vol. 21, no. 4, pp. 296–304, 2002.
- [6] J.-P. Thirion, “Non-rigid matching using demons,” in *Proceedings of IEEE Computer Vision and Pattern Recognition (CVPR)*, pp. 245–251, 1996.
- [7] I. Schoemaker, P. W. Hoefnagel, T. Mastenbroek, F. Kolff, S. Picken, F. T. van der Helm, and H. Simonsz, “Elasticity, viscosity and deformation of retrobulbar fat in eye rotation,” in *Proceedings of the Association for Research in Vision and Ophthalmology (ARVO) Annual Meeting*, 2003.
- [8] C. P. Botha, “DeVIDE: The Delft Visualisation and Image processing Development Environment,” tech. rep., Delft Technical University, 2004.
- [9] W. Schroeder, K. Martin, and B. Lorensen, *The Visualization Toolkit*. Prentice Hall PTR, 2nd ed., 1999.
- [10] L. Ibanez, W. Schroeder, L. Ng, and J. Cates, *The ITK Software Guide*. Kitware Inc., 2003.
- [11] G. Abram and L. Treinish, “An extended data-flow architecture for data analysis and visualization,” in *Proceedings of the 6th conference on Visualization '95*, p. 263, IEEE Computer Society, 1995.
- [12] C. Upton, T. Faulhaber, D. Kamins, D. Laidlaw, D. Schlegel, J. Vroom, R. Gurwitz, and A. van Dam, “The Application Visualization System: A Computational Environment for Scientific Visualization,” *IEEE Computer Graphics and Applications*, pp. 30–42, July 1989.
- [13] B. K. Horn, “Closed-form solution of absolute orientation using unit quaternions,” *Journal of the Optical Society of America A*, vol. 4, pp. 629–642, 1987.